Corrosion Behavior of Amorphous Nickel-Base Alloys in a Boiling Concentrated Sodium Hydroxide Solution

Corrosion Behavior of Amorphous Nickel-Base Alloys in a Boiling Concentrated Sodium Hydroxide Solution*

Kazuo SHIMAMURA**, Kimikado MIURA**, Asahi KAWASHIMA, Katsuhiko ASAMI and Koji HASHIMOTO

Institute for Materials Research

(Received January 31, 1987)

Synopsis

Polarization curves were measured in a boiling 50% NaOH solution, and the specimen surface was analyzed by X-ray photoelectron spectroscopy. A combined addition of chromium and molybdenum to amorphous nickel-phosphorus alloys significantly enhances the corrosion resistance. Addition of copper and lead are also effective in improving the corrosion resistance. The surface film formed on amorphous nickel-base alloys consists mainly of hydrated nickel oxyhydroxide. Chromium is concentrated in the alloy surface immediately under the surface film when nickel-base alloys containing chromium are immersed or polarized anodically at potentials close to the corrosion potential.

I. Introduction

Since extremely corrosion-resistant amorphous iron base alloys containing chromium were found[1], a number of corrosion-resistant amorphous alloys have been discovered[2]. Even in hot concentrated hydrochloric acids, some of the amorphous Fe-Cr-Mo-metalloid alloys become spontaneously passive[3]. Amorphous nickel-base alloys containing valve metals such as tantalum, possess a very high corrosion resistance in boiling concentrated nitric and hydrochloric acids[4,5].

The corrosion behavior of amorphous alloys in hot concentrated alkaline solutions, however, have not yet been studied. Sakaki and his coworkers have studied the corrosion behavior of crystalline metals in

---

* The 1834th report of Institute for Materials Research.

** Mitsui Engineering & Shipbuilding Co., Ltd. 1 Yawatakaigan-Dori, Ichihara, Chiba 290, Japan.

hot concentrated NaOH solutions, such as iron[6], Fe-Cr alloys[7,8] and Fe-Ni-Cr alloys[9-11]. The active dissolution of iron as FeO_2^{2-} and FeO_2^- in hot 48% NaOH solutions is suppressed by an addition of chromium, and an Fe-24 wt% Cr alloy does not show the active dissolution current in the solution at 140°C[7]. An addition of nickel to Fe-Cr alloys decreases the active dissolution current[9]. Since additions of both chromium and nickel decrease the active dissolution current of iron base alloys, the corrosion behavior of nickel-base alloys containing chromium is of interest.

The present work aims to find amorphous alloys which are stable in boiling concentrated sodium hydroxide solutions. The corrosion behavior have been investigated by polarization measurement and XPS analysis.

II. Experimental

Alloy ingots of about 50 compositions were prepared by induction melting of commercial metals and nickel phosphide and laboratory made cobalt phosphide. Phosphorus was added in the form of nickel phosphide or cobalt phosphide. The nickel phosphide was Ni-23.5 at% P. The cobalt phosphide was prepared similarly to palladium phosphide[12] by the reaction of cobalt powder and red phosphorus and was Co-22 at% P. Carbon was added in the form of chromium carbide which was Cr-32 at% C. The alloy ingot was prepared by sucking up the induction-melted alloy in a quartz tube followed by water quenching. Amorphous alloys were prepared under an argon atmosphere by the rotating wheel method using these alloy ingots. The formation of the amorphous structure was confirmed by X-ray diffraction using Cu Kα radiation. Since the chemical composition of the amorphous alloy prepared by rapid quenching from the liquid state is generally close to the nominal composition, alloys used in the present work are described by their nominal compositions in atomic percent except for lead-bearing alloys. The solubility of lead in nickel-base alloys is very low and the amorphous alloys are supersaturated with lead. Consequently, compositions of amorphous lead-bearing alloys were estimated by electron probe microanalysis (EPMA). Table 1 shows EPMA results of lead-bearing alloys along with some other alloys. Prior to electrochemical measurements alloy specimens were polished mechanically with silicon carbide paper up to No. 1000 in cyclohexane.

A solution used was a boiling 50 wt% NaOH solution (about 145°C) which was prepared by a reagent grade chemical and distilled water. Polarization curves were measured potentiodynamically with a potential

Table 1 Compositions of amorphous alloys (at%)

Alloy	Ni	Cr	Mo	Cu	Pb	P	C
Ni-Pb-20P	77.9				1.1	21.0	
Ni-5Cu-20P	75.41			3.80		20.79	
Ni-15Cr-5Mo-13P-7C	60.38	14.82	4.28			14.09	6.42
Ni-15Cr-5Mo-Pb-13P-7C	56.88	15.74	4.89		0.52	15.25	6.72
Ni-15Cr-5Mo-5Cu-Pb-13P-7C	52.96	15.59	4.71	4.61	0.83	14.59	6.70

sweep rate of 100 mV/min. An electrolytic cell used was made of PTFE. An Ag/AgCl/saturated KCl electrode was used as a reference electrode.

After immersion or potentiostatic polarization, X-ray photoelectron spectra from specimens were measured by SHIMADZU-ESCA 750 electron spectrometer with Mg $K\alpha$ excitation (1253.6 eV). Binding energies of electrons were calibrated by the method described elsewhere[13,14]. The composition and thickness of the surface film and the composition of the substrate alloy immediately under the surface film were quantitatively determined by the previously proposed method[15,16].

The quantitative determination was carried out using the assumption of a three-layer model of the outermost contaminant hydrocarbon layer of uniform thickness, the surface film of uniform thickness and the underlying alloy of X-ray photoelectron spectroscopically infinite thickness and the assumption of a homogeneous distribution of constituents in each layer. The photoionization cross-sections relative to the O 1s electrons used have been summarized elsewhere[17] except for copper. The most intense photoelectron spectrum of copper is the Cu $2p_{3/2}$. However, the chemical shift in the Cu $2p_{3/2}$ electrons between cuprous ion (Cu^+) in a surface film and metallic copper (Cu^M) in its substrate metal is not large, although the Cu^{2+} $2p_{3/2}$ spectrum is separated from the Cu^M $2p_{3/2}$ spectrum. On the other hand the X-ray induced Cu $L_3M_{4,5}M_{4,5}$ Auger electron spectrum shows the clear chemical shift between Cu^{ox} and Cu^M. Accordingly both the Cu $2p_{3/2}$ and Cu $L_3M_{4,5}M_{4,5}$ Auger spectra were used for the qualitative and quantitative determinations[18]. The measured spectrum of an element was separated into spectra originating from respective components of different valences in a manner similar to the separation method of the Fe $2p_{3/2}$ spectrum into Fe^{3+}, Fe^{2+} and Fe^M components[19].

III. Results

1. Polarization curves

Figure 1 shows polarization curves of amorphous nickel-metalloid and cobalt-metalloid alloys measured in a boiling 50 % NaOH solution. The cobalt base alloy shows a very low corrosion potential and a very high anodic dissolution current. It seems, therefore, difficult to improve the corrosion resistance of the cobalt-base alloy by alloying. By contrast, amorphous nickel-metalloid alloys show higher corrosion potentials and lower anodic current densities. A comparison of two Ni-Si-B alloys reveals that increasing silicon content increases the anodic current density and lowers the corrosion potential, suggesting a detrimental effect of increasing silicon content for the corrosion resistance in the boiling concentrated sodium hydroxide solution. Since the Ni-20P alloy shows the lowest maximum current density in the active region among alloys shown in Figure 1, an improvement of the corrosion resistance by alloying was attempted by using the Ni-20P alloy. However, since phosphorus was added in the form of nickel-phosphide, the alloy phosphorus content was sometimes lower than 20 at% due to a decrease in nickel content of an alloy as a result of alloying with other elements.

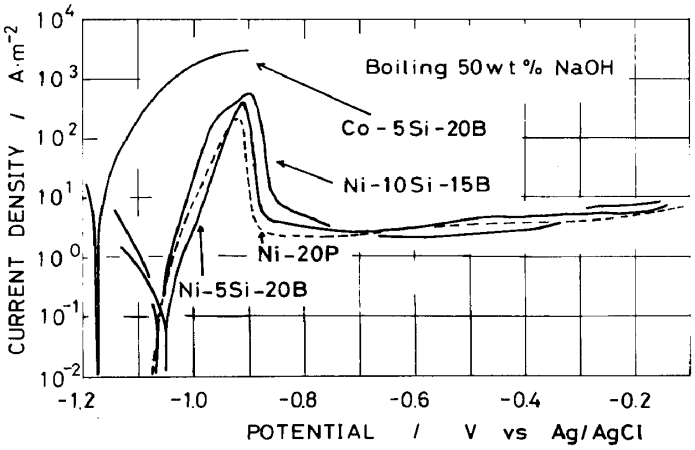

Fig. 1 Polarization curves of amorphous alloys measured in a boiling 50% NaOH solution.

Figure 2 shows the effect of chromium addition on polarization curves. Increasing chromium content ennobles the corrosion potential and decreases the current density in the active region. Accordingly the chromium addition is effective in enhancing the corrosion resistance. However, alloys containing 25 and 30 at% chromium exhibit no clear passivation and show high current densities in the passive region of lower chromium alloys.

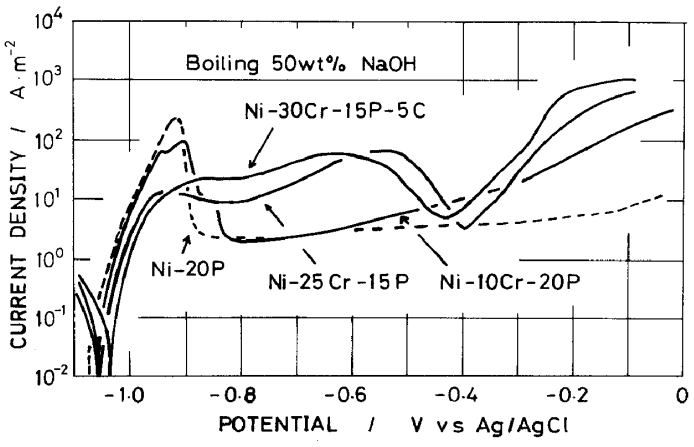

Fig. 2 Polarization curves of amorphous alloys measured in a boiling 50% NaOH solution.

The addition of molybdenum to amorphous nickel-met-

alloid alloys improves the corrosion resistance in acids[20]. However, as shown in Figure 3, the molybdenum addition increases anodic current densities and hence is rather detrimental in the boiling concentrated NaOH solution, although the corrosion potential is slightly ennobled. By contrast, a combined addition of chromium and molybdenum to amorphous nickel-metalloid alloys is quite effective in enhancing the corrosion resistance. As shown in Figure 4, the alloy containing both chromium and molybdenum has a significantly high corrosion potential and a low active dissolution current. Although the alloy containing both chromium and molybdenum shows a higher current density in the passive region, the open circuit corrosion rate seems considerably lower in comparison with amorphous Ni-20P, Ni-15Cr-20P and Ni-5Mo-20P alloys.

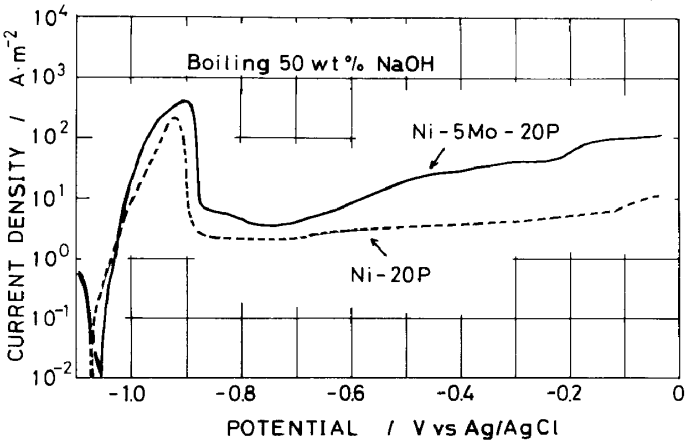

Fig. 3 Polarization curves of amorphous alloys measured in a boiling 50% NaOH solution.

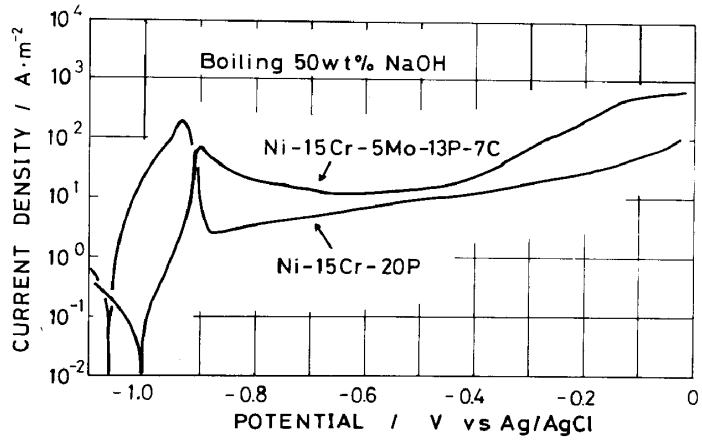

Fig. 4 Polarization curves of amorphous alloys measured in a boiling 50% NaOH solution.

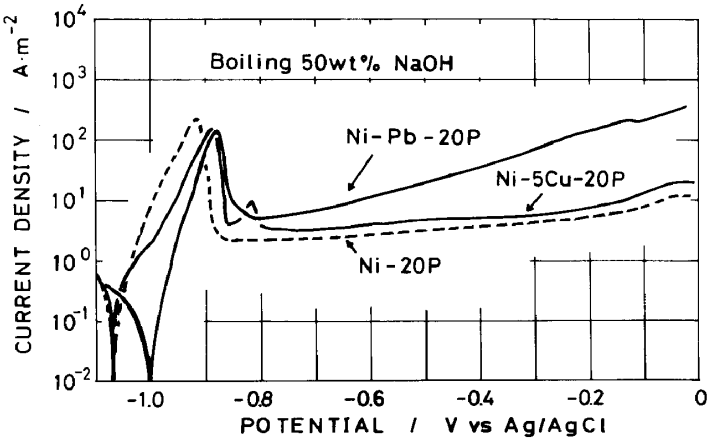

Fig. 5 Polarization curves of amorphous alloys measured in a boiling 50% NaOH solution.

On the other hand, the addition of a small amount of lead to the amorphous Ni-20P alloy ennobles largely the corrosion potential and decreases the anodic dissolution current as shown is Figure 5. The addition of copper to the Ni-20P alloy also decreases the anodic

dissolution current although the copper addition is not effective for an ennoblement of the corrosion potential.

Since additions of chromium, molybdenum, lead and copper to amorphous nickel-metalloid alloys are effective in improving the corrosion resistance in the boiling concentrated alkaline solution, polarization curves of alloys containing these elements were measured and are shown in Figure 6. The amorphous Ni-15Cr-5Mo-5Cu-Pb-13P-7C alloy has a high corrosion potential and a low active dissolution current, and hence has the highest corrosion resistance among alloys examined.

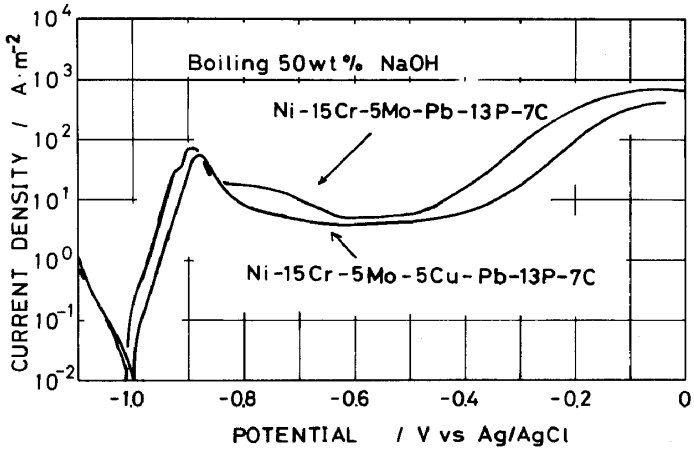

Fig. 6 Polarization curves of amorphous alloys measured in a boiling 50% NaOH solution.

2. Analytical Results by XPS

For a better understanding of the polarization behavior, an XPS analysis was applied to some typical alloys after immersion or potentiostatic polarization in the boiling 50% NaOH solution.

The spectra over the wide binding energy region exhibited peaks of oxygen and carbon as well as those of alloy constituents. The C 1s spectrum found arose from a contaminant hydrocarbon layer covering the specimen surface[21]. All spectra from alloy constituents were composed of superposed two spectra corresponding to oxidized state (ox) in the surface film and the metallic state (M) in the alloy surface immediately under the surface film. The binding energies of Ni^{ox} and Ni^{M} $2p_{3/2}$ electrons were 856.6-856.9 and 853.0-853.3 eV, respectively, and hence the nickel ion in the surface film was assigned to Ni^{2+} ion. The binding energies of Cr^{ox} and Cr^{M} $2p_{3/2}$ electrons were 573.3-573.4 and 577.3-577.4 eV, respectively, and hence the chromium ion in the surface film was assigned to Cr^{3+} ion. The Mo^{ox} $3d_{3/2}$ and Mo^{M} $3d_{5/2}$ electrons showed peaks at about 236 and 228 eV, respectively. The Mo^{ox} was assigned to Mo^{6+} ion. Because of a very low concentration of lead, Pb^{M} 4f signal was not detected. The Pb^{ox} $4f_{7/2}$ electrons showed a peak at 139.2-139.4 eV. Standard PbO and Pb metal gave the Pb $4f_{7/2}$ peak at 138.8 and 136.8 eV, respectively. However, since the peak binding energy of Pb^{4+} $4f_{7/2}$ electrons is very close to the Pb^{2+} $4f_{7/2}$ electrons, the valencee of the Pb^{ox} in the surface film was not estimated. The Cu $L_3M_{4,5}M_{4,5}$ Auger electron spectrum showed the presence of Cu^{ox}

and Cu^M, and the Cu $2p_{3/2}$ spectrum exhibited no signal of the Cu^{2+} $2p_{3/2}$ electrons. Hence the copper ion in the surface film was assigned to Cu^+ ion. The P 2p spectra showed two peaks at 133.3-133.9 and 129.7-130.1 eV, respectively. The high binding energy peak was assigned to P^{5+} 22) in phosphate in the surface film. The O ls spectrum was considerably wide because it arose from oxygen in O^{2-}, OH^-, PO_4^{3-} and H_2O.

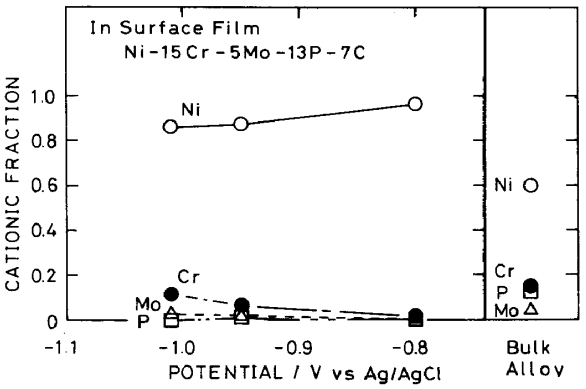

Fig. 7 Cationic fractions in the surface film formed on an amorphous Ni-15Cr-5Mo-13P-7C alloy in a boiling 50% NaOH solution.

After integrated intensities of photoelectron spectra were separately obtained for individual species, the quantitative determination of the thickness and composition of the surface film and the composition of underlying alloy was performed. Figure 7 shows fractions of cations in the surface film formed on the amorphous Ni-15Cr-5Mo-13P-7C alloy by immersion and potentiostatic polarization in the boiling 50% NaOH solution. The surface film is significantly rich with nickel ion and deficient with ions of other alloy constituents. The surface film formed by immersion contains some chromic ions, but the ratio of chromic ion to nickel, 0.128, is almost a half of the Cr/Ni ratio of 0.245 in the underlying bulk alloy. Since O^{2-}, OH^- and H_2O are contained in the surface film the surface film is composed mainly of hydrated nickel oxyhydroxide. Figure 8 shows atomic fractions in the alloy surface immediately under the surface film. The chromium enrichment is significant particularly under the open circuit condition. Accordingly, when nickel-base alloys containing chromium is immersed in the boiling 50% NaOH solution nickel dissolves rapidly as well as molybdenum, phosphorus and carbon. Since the reaction rate of chromium in this solution is slower than other alloy constituents, chromium becomes concentrated in the alloy surface just under the surface film. Consequently, nickel is not a stable element in the boiling 50% NaOH solution although a hy-

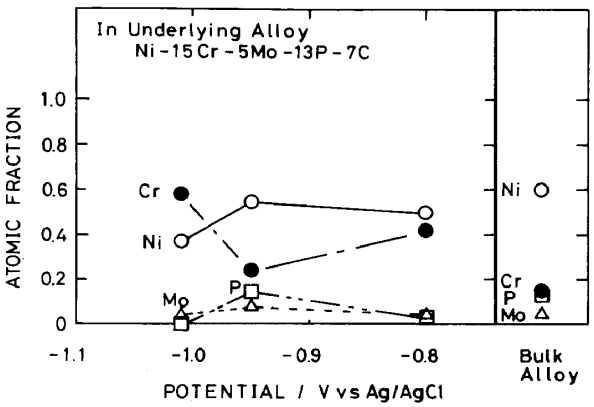

Fig. 8 Atomic fractions in the alloy surface immediately under the surface film formed on an amorphous Ni-15Cr-5Mo-13P-7C alloy in a boiling 50% NaOH solution.

drated nickel oxyhydroxide film is formed, and the formation of the alloy surface in which less reactive chromium is concentrated is responsible for a lower dissolution current and a higher corrosion potential of chromium containing alloys.

Figure 9 shows fractions of cations in the surface film formed on the amorphous Ni-Pb-20P alloy in the boiling 50% NaOH solution, and Figure 10 gives atomic fractions in the alloy surface just below the surface film. In spite of a low lead content of the alloy lead ion is contained in the surface film, the major cation in the surface film is Ni^{2+}, and the surface film consists of hydrated nickel oxyhydroxide containing some phosphate and lead ion.

Figure 11 shows fractions of cations in the surface film formed on the amorphous Ni-5Cu-20P alloy in the boiling 50% NaOH solution and Figure 12 show atomic fractions in the alloy surface immediately under the surface film. At -950 mV where the suppression of anodic current density by the copper addition was most remarkable as shown in Figure 5 copper is enriched both in the surface film and underlying alloy surface. At -900 mV where the beneficial effect of the copper addition for a decrease in anodic current density is still observed, the surface film is rich with cuprous ion.

Figure 13 shows cationic fractions in the surface film

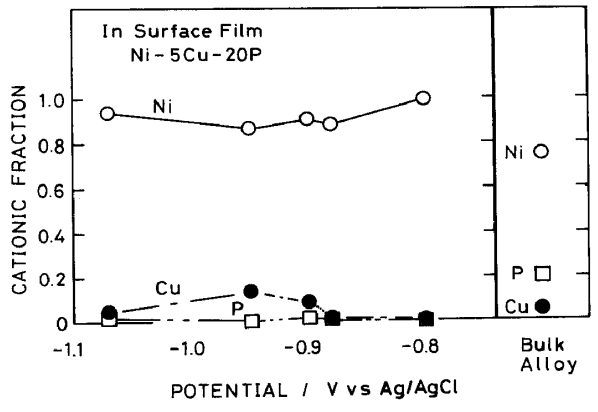

Fig. 11 Cationic fractions in the surface film formed on an amorphous Ni-5Cu-20P alloy in a boiling 50% NaOH solution.

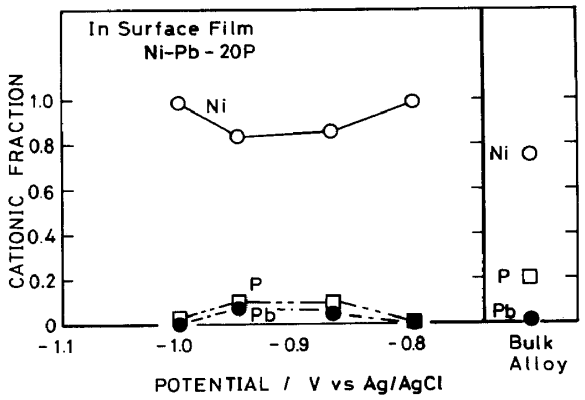

Fig. 9 Cationic fractions in the surface film formed on an amorphous Ni-Pb-20P alloy in a boiling 50% NaOH solution.

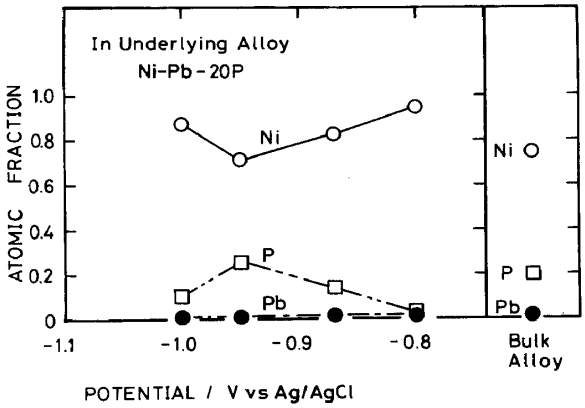

Fig. 10 Atomic fractions in the alloy surface immediately under the surface film formed on an amorphous Ni-Pb-20P alloy in a boiling 50% NaOH solution.

formed on the amorphous Ni-15Cr-5Mo-5Cu-Pb-13P-7C alloy in the boiling 50% NaOH solution and Figure 14 exhibits atomic fractions of the alloy surface immediately under the surface film. The main cations in the surface film are nickel ions, and some chromium ions are also found. However, cationic fractions of other alloy constituents are very low and are less than 0.006. Thus only fractions of Ni^{2+} and Cr^{3+} ions are shown in Figure 13. Figure 13 simply exhibits that the surface film consists mainly of hydrated nickel oxyhydroxide containing a small amount of chromic ion. The thickness of the surface film is not thin and ranges from 6 to 7 nm, suggesting that its protective quality is lower than the passive film. On the other hand, chromium is concentrated in the underlying alloy surface particularly at low potentials including the open circuit potential.

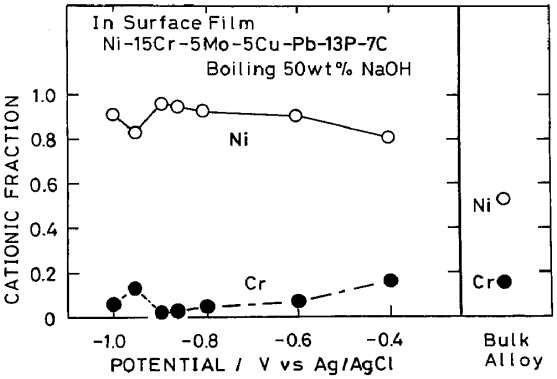

Fig. 13 Cationic fractions in the surface film formed on an amorphous Ni-15Cr-5Mo-5Cu-Pb-13P-7C alloy in a boiling 50% NaOH solution.

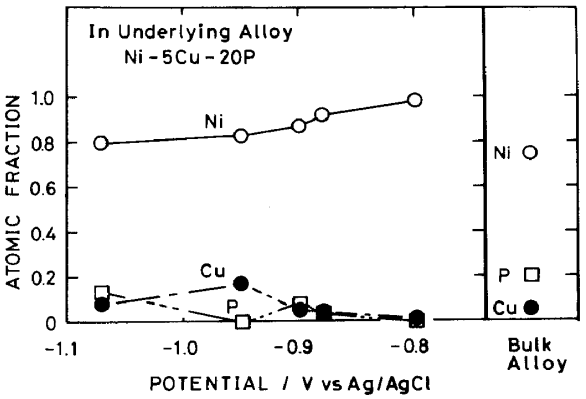

Fig. 12 Atomic fractions in the alloy surface immediately under the surface film formed on an amorphous Ni-50Cu-20P alloy in a boiling 50% NaOH solution.

Consequently, nickel forms the hydrated nickel oxyhydroxide film in the boiling 50% NaOH solution but nickel dissolves considerably rapidly since it is not a stable element in this solution. Chromium added to the nickel-base alloys has the lowest reactivity among various alloying elements examined and is concentrated in the alloy surface just below the surface film as a result of selective dissolution of various elements such as nickel, molybdenum, copper, lead, phosphorus and carbon.

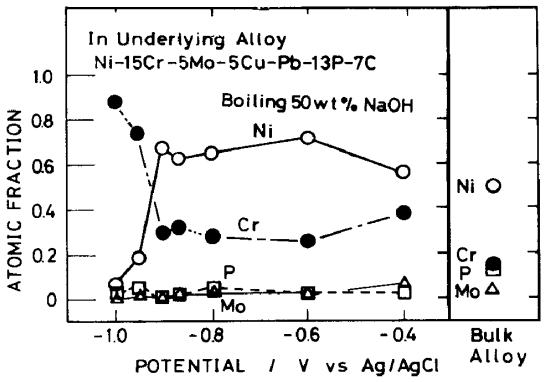

Fig. 14 Atomic fractions in the alloy surface immediately under the surface film formed on an amorphous Ni-15Cr-5Mo-5Cu-Pb-13P-7C alloy in a boiling 50% NaOH solution.

IV. Conclusions

In order to find alloys having a high corrosion resistance in a very aggressive and special environment, i.e. a boiling 50% NaOH solution, the corrosion behavior of various amorphous alloys prepared by rapid quenching from the liquid state was examined by polarization measurement and XPS analysis. The following conclusions were drawn:

1. Nickel-metalloid alloys have better corrosion resistance than a cobalt-metalloid alloy.
2. A combined addition of chromium and molybdenum to a nickel-phosphorus alloy significantly improves the corrosion resistance.
3. Additions of copper and lead to the nickel-phosphorus alloy are also effective in enhancing the corrosion resistance.
4. The alloy containing all these elements mentioned above, such as an amorphous Ni-15Cr-5Mo-5Cr-Pb-13P-7C alloy shows the highest corrosion potential and the lowest active dissolution current among alloys examined.
5. XPS analysis reveals that the surface film formed on amorphous nickel-base alloys in the boiling 50% NaOH solution consists mainly of hydrated nickel oxyhydroxide.
6. Chromium is concentrated in the alloy surface just below the surface film after immersion or polarization at potentials near the corrosion potential possibly due to the lowest reactivity of chromium among alloy constituents examined in the boiling concentrated NaOH solution.

Acknowledgement

Financial supports of Grant-in-Aid for Developmental Scientific Research No. 61850127 from the Ministry of Education, Science and Culture is greatly acknowledged.

References

(1) M. Naka, K. Hashimoto and T. Masumoto, J. Japan Inst. Metals, 38 (1974), 835.

(2) K. Hashimoto, "Rapidly Quenched Metals", S. Steeb and H. Warlimont, Eds. Elsevier, Amsterdam (1985), Vol. 2, p. 1449, p. 1109.

(3) K. Hashimoto, K. Kobayashi, K. Asami and T. Masumoto, Proc. 8th Int. Cong. Metallic Corrosion, DECHEMA, Frankfurt (1981), Vol. I, p. 70.

(4) A. Kawashima, K. Shimamura, S. Chiba, T. Matsunaga, K. Asami and K. Hashimoto, Proc. Asian-Pacific Corrosion Control. Conf., Tokyo (1985), Vol. 2, p. 1042.
(5) K. Shimamura, A. Kawashima, K. Asami and K. Hashimoto, Sci. Rep. RITU, A33 (1986), 196.
(6) H. Onoe, T. Sakaki and K. Sakiyama, J. Japan Inst. Metals, 43 (1979) 258.
(7) T. Sakaki and K. Sakiyama, J. Japan Inst. Metals, 43 (1979), 527.
(8) T. Sakaki and K. Sakiyama, J. Japan Inst. Metals, 43 (1979), 1186.
(9) T. Sakaki and K. Sakiyama, J. Japan Inst. Metals, 44 (1980), 582.
(10) T. Sakaki, Y. Shimizu and K. Sakiyama, J. Japan Inst. Metals, 45 (1981) 296.
(11) T. Sakaki and K. Sakiyama, J. Japan Inst. Metals, 49 (1985) 209.
(12) M. Hara, K. Asami, K. Hashimoto and T. Masumoto, Electrochim. Acta, 31 (1986), 481.
(13) K. Asami, J. Electron Spectrosc., 9 (1976) 469.
(14) K. Asami and K. Hashimoto, Corros. Sci., 17 (1977), 559.
(15) K. Asami, K. Hashimoto and S. Shimodaira, Corros. Sci., 17 (1977), 713.
(16) K. Asami and K. Hashimoto, Corros. Sci., 24 (1984), 83.
(17) K. Hashimoto and K. Asami, Corros. Engng. (Boshoku Gijutsu), 26 (1977), 375.
(18) K. Asami and K. Hashimoto, Trans. Japan Inst. Metals, 20 (1979), 119.
(19) K. Asami, K. Hashimoto and S. Shimodaira, Corros. Sci., 16 (1976), 387.
(20) A. Kawashima, K. Asami and K. Hashimoto, J. Non-Cryst. Solids, 70 (1985), 69.
(21) K. Siegbahn, C. Nordling, A. Fahlman, R. Nordberg, K. Hamrin, J. Hedman, G. Johansson, T. Bergmark, S. E. Karlson, I. Lindgren and B. Lindberg, "ESCA-Atomic, Molecular, and Solid State Structure Studied by Means of Electron spectroscopy", Nova Acta Regiae, Soc. Sci. Upsalinsis, Ser IV, Vol.20, 1967.
(22) M. Pelavin, D. N. Henderson, J. M. Hollander and W. Z. Jolly, J. Phys. Chem. 74 (1976), 1116.